Osteoarthritis and Cartilage 20 (2012) 184–190

Osteoarthritis and Cartilage

Spin–lattice relaxation rates and water content of freeze-dried articular cartilage

R.A. Damion †, S.S. Pawaskar ‡, M.E. Ries †[a], E. Ingham §, S. Williams ‡, Z. Jin ‡, A. Radjenovic ‖*[a]

† School of Physics & Astronomy, University of Leeds, Leeds LS2 9JT, UK
‡ Institute of Medical and Biological Engineering, School of Mechanical Engineering, University of Leeds, Leeds LS2 9JT, UK
§ Institute of Molecular & Cellular Biology, Faculty of Biological Sciences, University of Leeds, Leeds, LS2 9JT, UK
‖ NIHR Leeds Musculoskeletal Biomedical Research Unit and Leeds Institute of Molecular Medicine, University of Leeds, Chapel Allerton Hospital, Leeds LS7 4SA, UK

ARTICLE INFO

Article history:
Received 15 August 2011
Accepted 12 December 2011

Keywords:
Articular cartilage
MRI
Spin–lattice relaxation
Longitudinal relaxation
Water content
Freeze-drying

SUMMARY

Objective: Nuclear magnetic resonance (NMR) spin–lattice relaxation rates were measured in bovine and porcine articular cartilage as a function of water content.
Methods: Water content was varied by freeze-drying samples for short periods of time (up to 15 min). The samples were weighed at all stages of drying so that water content could be quantified. Spin–lattice relaxation rates were measured using magnetic resonance imaging (MRI).
Results: Linear correlations were observed between relaxation rate and two measures of inverse water content: (1) solid-to-water ratio (ρ), expressed as a ratio of the mass of the solid component of the cartilage (m^s) and the mass of water at each freeze-drying time point (m^w), and (2) a ratio of the total mass of the fully-hydrated cartilage and m^w ($1/w$). These correlations did not appear significantly different for the bovine and porcine data. However, fitting the data to a piecewise-linear model revealed differences between these two species. We interpret the first two segments of the piecewise model as the depletion of different water phases but conjecture that the third segment is partially caused by changes in relaxation rates as a result of a reduction in macromolecular mobilities.
Conclusions: Whilst we can produce linear correlations which broadly describe the dependence of the measured spin–lattice relaxation rate on (inverse) water content, the linear model seems to obscure a more complicated relationship which potentially provides us with more information about the structure of articular cartilage and its extracellular water.

Introduction

There is currently much interest in studying the properties of articular cartilage in terms of its biomechanical and tribological behaviour[1–4]. There is also interest in determining its nuclear magnetic resonance (NMR) properties so that useful information can be obtained using magnetic resonance imaging (MRI) in a clinical setting[5,6] as well as *ex vivo* or *in vitro*.

Since articular cartilage is a biphasic material, its mechanical properties are dependent on its state of hydration. Therefore, the water content is one of the basic constitutive parameters of importance in cartilage. The biomechanical properties of cartilage are primarily defined by two components of its extracellular matrix: the fibrillar collagen network and negatively charged proteoglycan molecules[7–9]. Fibrillar network disruption or proteoglycan depletion has a direct impact on cartilage water content, distribution and re-distribution under loading. The exact nature of the interplay between the pathological changes that are present in degenerative osteoarthritis is still the subject of intensive ongoing research. However, the changes in water content that occur as a result of these pathological processes are well recognised[10].

Water content is also the primary source of image intensity in MR images. Not only is the intensity directly proportional to the hydration level of the tissue but relaxation times and diffusion coefficients (which modify the image intensity) are also affected by the water content.

Besides water content, MRI can be used to assess other important factors that reflect biochemical and biomechanical properties of cartilage. Most notably, delayed gadolinium MRI of cartilage (dGEMRIC) provides a powerful tool to assess glycosaminoglycan (GAG) content within a clinical setting[11]. Emerging methods for morphological cartilage assessment using accelerated clinical three-dimensional (3D) sequences on clinical 3T MRI systems also show a great deal of promise[12].

* Address correspondence and reprint requests to: Aleksandra Radjenovic, NIHR Leeds Musculoskeletal Biomedical Research Unit, University of Leeds, Chapel Allerton Hospital, Leeds LS7 4SA, UK. Tel: 44-113-392-4482.
E-mail address: a.radjenovic@leeds.ac.uk (A. Radjenovic).
[a] Equal contribution.

1063-4584/$ – see front matter
doi:10.1016/j.joca.2011.12.005

One method of investigating the mechanical properties of cartilage is by subjecting samples to compression experiments and monitoring temporal changes. The obvious consequence of compressing cartilage is that its hydration state changes. These changes should affect NMR parameters and thus the appearance of MR images[13,14].

It is possible to use MRI to measure a quantity closely related to water content, namely, proton density. Measuring this quantity would be the most direct manner of estimating the water content of a sample but such measurements tend to require longer imaging times than needed to measure relaxation rates and often require the presence of a calibration substance (usually water). Since the faster imaging method is favourable in the measurement of temporally changing quantities, we considered the measurement of a relaxation rate instead of proton density.

Spin–spin relaxation is usually considered to be more sensitive to water content than spin–lattice relaxation but, in articular cartilage, the former suffers from the well-known[15,16] complication of being strongly dependent on collagen fibre orientation (with respect to the main magnetic field). Spin–lattice quantitation is also non-trivial (as it requires multiple measurements which are acquired in the presence of noise, possible magnetic field inhomogeneities and temperature fluctuations), but importantly it does not possess this orientational dependence.

Therefore, we have chosen to investigate the relationship between the water content of articular cartilage and spin–lattice relaxation rate, R_1, which has been shown to be correlated to some extent with water content[17].

In this work, we do not subject cartilage samples to compression but alter their water content by freeze-drying. Water content is obtained directly by weighing the samples between freeze-drying sessions and R_1 is measured using MRI. In doing this, our primary objective was to produce data which is useful in MRI studies of cartilage loading and recovery.

Method

Freeze-drying

Cartilage pins together with the subchondral bone were extracted, using a custom-made plug extractor, from the patello-femoral joint of healthy 18-month-old cows (within 72 h of slaughter) and 6-month-old pigs (within 36 h of slaughter) — see Table I. The cartilage pin was kept hydrated upon removal using phosphate buffered saline (PBS). PBS was prepared according to the manufacturer's recommendation (MPBio; Catalogue number: 2810305). Cartilage was then removed from the bone using a scalpel and stored at −20°C, wrapped in a PBS-soaked tissue, in a bijou container. Prior to their use, the samples were defrosted in a warm water bath for at least an hour (sealed within their bijou).

The weight of each bijou was recorded with and without cartilage samples prior to freeze-drying. The difference in weight gave the initial weight of each sample. The samples were placed in a freeze-drier (ModulyoD-230, Thermo Scientific) for various durations (see Table I) and subsequently imaged. At each stage, the combined weight of the bijou and sample was recorded. The freeze-dryer operated at approximately −55°C. Time in the freeze-dryer was counted from the time the pressure reached 1.2 mbar until the pump was stopped manually, which after approximately 2.5 min was about 750 μbar. Finally, all samples were placed in the freeze-dryer for complete drying (for a total of approximately 65 h) to obtain the dry weight.

Table I
Cartilage samples and drying times. All samples were 1–1.5 mm thick

Sample	Diameter [mm]	Drying times [min]
Porcine P1	9	0, 5, 10, 15
Porcine P2	6	0, 2.5, 5, 7.5, 10, 12.5, 15
Porcine P3	6	0, 2.5, 5, 7.5, 10, 12.5
Porcine P4	6	0, 2.5, 5, 7.5, 10, 12.5
Bovine B1	6	0, 2.5, 5, 7.5, 10, 12.5, 15
Bovine B2	6	0, 2.5, 5, 7.5, 10, 12.5, 15
Bovine B3	6	0, 2.5, 5, 7.5, 10, 12.5

Two measures were used to quantify water content. The solid-to-water ratio, was defined by

$$\rho = \frac{m^{\mathrm{s}}}{m^{\mathrm{w}}} \tag{1}$$

where m^{w} is the mass of water (which is understood to be a function of drying time t), and m^{s} is the mass of the solid component of the cartilage (assumed independent of drying time). The second measure of water content was defined as

$$w = \frac{m^{\mathrm{w}}}{m_0^{\mathrm{w}} + m^{\mathrm{s}}} \tag{2}$$

where m_0^{w} is the mass of water of the fully-hydrated cartilage. These two quantities are related by

$$\frac{1}{w} = \rho\left(1 + \frac{1}{\rho_0}\right) \tag{3}$$

where ρ_0 is the fully-hydrated solid-to-water ratio. The fully-hydrated water content can thus be found from $1/w_0 = 1 + \rho_0$.

T_1 measurements

All MRI measurements were performed on a Bruker (Bruker Biospin MRI GmbH) Avance II microimaging (vertical bore) system operating at 400 MHz.

Saturation-recovery sequence

T_1 measurements were performed using a saturation-recovery sequence by MRI. T_{R} values of 200, 400, 700, 1400, 2600, and 5000 ms were used (as were used by Berberat *et al.*[17]) and each pixel in the resulting image set was fitted to the equation,

$$M(T_{\mathrm{R}}) = M_{\mathrm{eq}}\left(1 - e^{-T_{\mathrm{R}}/T_1}\right) \tag{4}$$

to obtain T_1 and M_{eq}. The latter quantity is T_2-weighted with an echo time of 12.5 ms. Samples were oriented (as much as possible) such that the normal to the surface was parallel to the main magnetic field direction. The (coronal) slice thickness was usually 2 mm, and the pixel resolution was 70 μm × 70 μm. The number of averages was varied depending on the appearance of images during the experiments.

The cartilage samples were imaged in groups. Sample P1 was imaged by itself. Samples P2, B1, and B2 were imaged as a group, as were samples P3, P4, and B3 (see Table I). All T_1 measurements were carried out at approximately 20°C.

Calculation of relaxation quantities

Using equation 4, images were derived for parameters T_1 and M_{eq}. An image was also produced for the goodness-of-fit (coefficient of determination), r^2, given by

$$r^2 = 1 - \frac{S_{\mathrm{res}}}{S_{\mathrm{tot}}} \tag{5}$$

where S_{tot} is the sum of squares of the y-data around the mean (proportional to the sample variance), and S_{res} is the sum of the square residuals in the y-data.

Relaxation quantities were calculated by averaging over several pixels in the T_1 image. This was achieved by identifying cartilage pixels which met three criteria. Firstly, values for the mean and standard deviation of the background noise were obtained for the M_{eq} image. Candidate pixels were then identified in this image by selecting values which were some number n_{std} of standard deviations above the mean background noise level in the image. This number was usually set to five. Secondly, pixels were rejected if $T_1 > 5$ s or $r^2 < 0.9$. Since we do not expect to observe spin–lattice relaxation times longer than that of PBS (for which we measure a relaxation time of 3.7 s) plus some allowance for noise, the T_1 threshold was set to 5 s. That is, any T_1 value greater than this was regarded as unphysical and this pixel was rejected.

Three different relaxation quantities were then calculated; $\langle T_1 \rangle$, $\langle R_1 \rangle$, and $\langle R_1 \rangle_w$. The first two quantities are the T_1 and $R_1 = 1/T_1$ averaged over all valid image pixels. The third quantity is a weighted average of R_1, weighted with the corresponding equilibrium magnetization;

$$\langle R_1 \rangle_w = \frac{\sum_{i=1}^{n} M_{eq} R_1}{\sum_{i=1}^{n} M_{eq}} \quad (6)$$

where n is the number of valid pixels. This quantity was chosen because it mimics a fast-exchange average of R_1 in different environments.

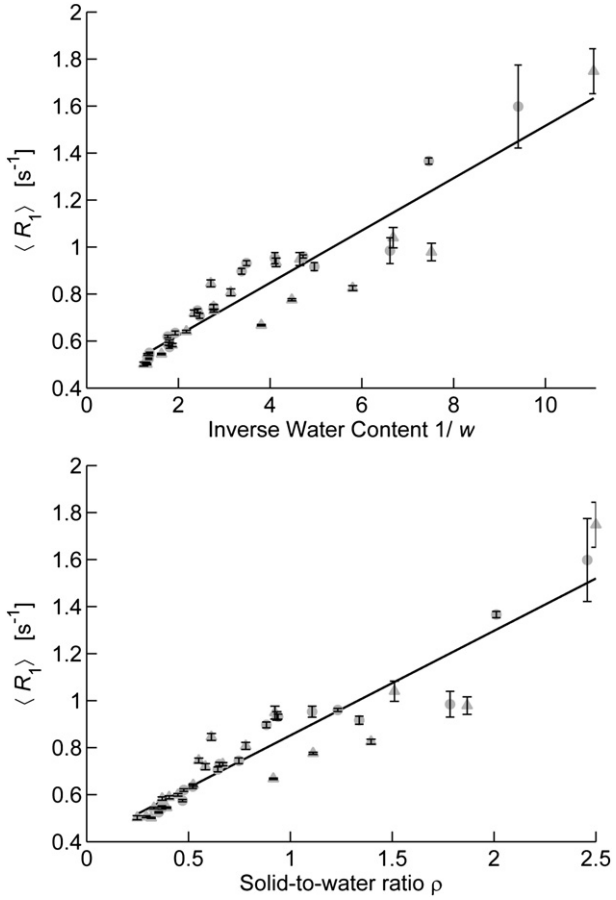

Fig. 1. $\langle R_1 \rangle$ against inverse water content and solid-to-water ratio. Bovine: ○, Porcine: △. Error bars represent 95% confidence intervals of the mean $\langle R_1 \rangle$ measured at each given $1/w$ or ρ value.

Results

Figure 1 shows data and linear regression lines for all data (bovine and porcine) for $\langle R_1 \rangle$ against two measures of water content. The data for the other relaxation quantities ($1/\langle T_1 \rangle$ and $\langle R_1 \rangle_w$) were very similar to those of $\langle R_1 \rangle$ and are not plotted but all regression data can be seen in Table II.

The regressions suggest that $\langle R_1 \rangle$ is linearly-dependent on the solid-to-water ratio and the inverse water content $1/w$ over a significant range of hydration level. This is consistent with a fast-exchange model of relaxation (see appendix) and the relation given in equation 3. It also appears from these plots that the bovine and porcine data are not significantly different.

Note that the intercepts in Table II are all consistent with a free-water relaxation time of approximately 2.5 s, which is a little lower than the measured value of PBS of approximately 3.7 s. From the slopes given in Table II, and since the slopes should differ by a factor of $1 + 1/\rho_0$ (see Appendix equations A.8 and A.9), an average value of ρ_0 can be calculated of 0.33, or a value $w_0 = 0.75$, consistent with the average initial water contents of the individual samples.

Berberat *et al.*[17] have previously correlated water content of (fully-hydrated) articular cartilage samples with spin–lattice relaxation rate, R_1 (also at 400 MHz spectrometer frequency). They used a measure of water content corresponding to w, but correlated R_1 directly with w instead of its inverse. If the data in Fig. 1 is plotted in this manner, a clear deviation from linearity is seen for w below approximately 0.14 (see Fig. 2). However, performing a linear regression on data in the apparent linear region we obtain similar results; intercept 1.05 s^{-1} and slope −0.75 s^{-1} (compared to Berberat *et al.*'s intercept 1.1 s^{-1} and slope −0.8 s^{-1}). In Fig. 2, we have also shown the corresponding plot for $1/\rho$, which displays the non-linearity a little more clearly throughout the range of values.

In Fig. 1 we did not separate the results for bovine and porcine data because, when plotted together or fitted separately with a linear regression model, there appears to be no significant difference between the cartilage of different species. However, if deviations from linearity are considered then differences do appear. In Fig. 3 we have separated the two species and fitted a piecewise-linear model (plotted against ρ only). Results for this fitting can be seen in Table III.

The piecewise-linear model consisted of three linear segments constrained such that the segments intercept at positions ρ_1 and ρ_2 with $\rho_1 \leq \rho_2$ and such that both segment intercepts lie within the range of the data. A non-linear least-squares fitting procedure was used to obtain the six parameters. We found it convenient to chose the parameters to be the three ($\rho = 0$) intercepts c_i, the two segment intercept positions ρ_j, and one of the three slopes m_0. The other two slopes are calculated directly from these parameters. Because the linear model is a sub-model of the piecewise-linear model we can easily perform an F-test to decide whether the latter model fits the data better. Table IV shows a comparison of the goodness-of-fit, r^2, and the F-value (based on the sum of the square residuals, S_{res}, and the degrees of freedom, d_f) for the two models. The final column of Table IV gives the P-value for the F-test and is a measure of the likelihood that the improved fitting of the piecewise-linear model is a result of scatter in the data. The P-values clearly indicate that the

Table II
Linear regression data. For all regressions $P < 0.0001$. Intercepts and slopes are in units [s^{-1}]

	$1/w$			ρ		
	Intercept	Slope	r^2	Intercept	Slope	r^2
$1/\langle T_1 \rangle$	0.389	0.098	0.828	0.394	0.391	0.815
$\langle R_1 \rangle$	0.402	0.111	0.887	0.407	0.445	0.877
$\langle R_1 \rangle_w$	0.385	0.110	0.881	0.390	0.441	0.870

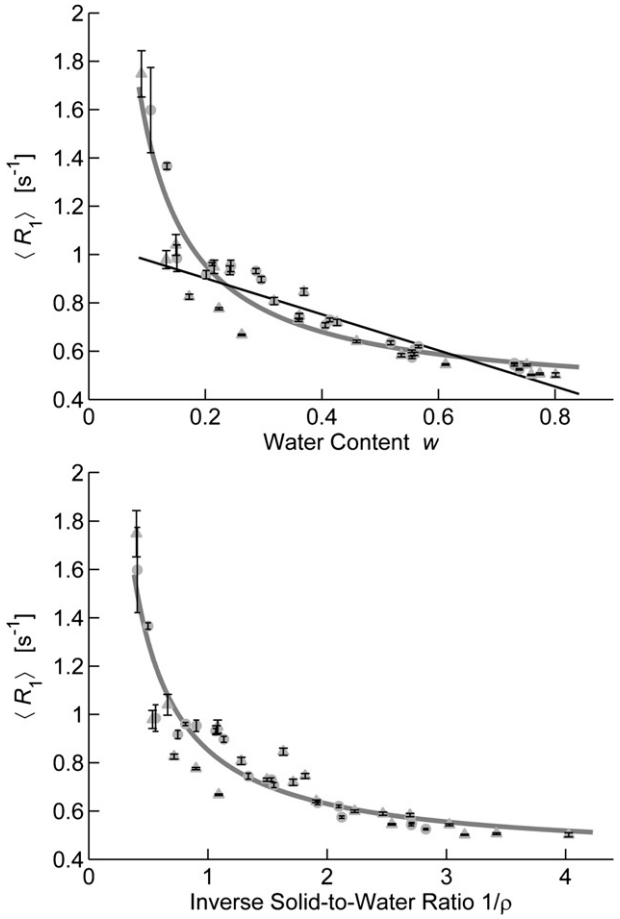

Fig. 2. $\langle R_1 \rangle$ against water content and inverse solid-to-water ratio. The thin black line (top graph) is the linear regression for $\langle R_1 \rangle < 1.2$. The grey lines are the predictions from the linear regression of $\langle R_1 \rangle$ against $1/w$ and $\langle R_1 \rangle$ against ρ. Bovine: ○, Porcine: △. Error bars represent 95% confidence intervals of the mean $\langle R_1 \rangle$ measured at each given $1/w$ or ρ value.

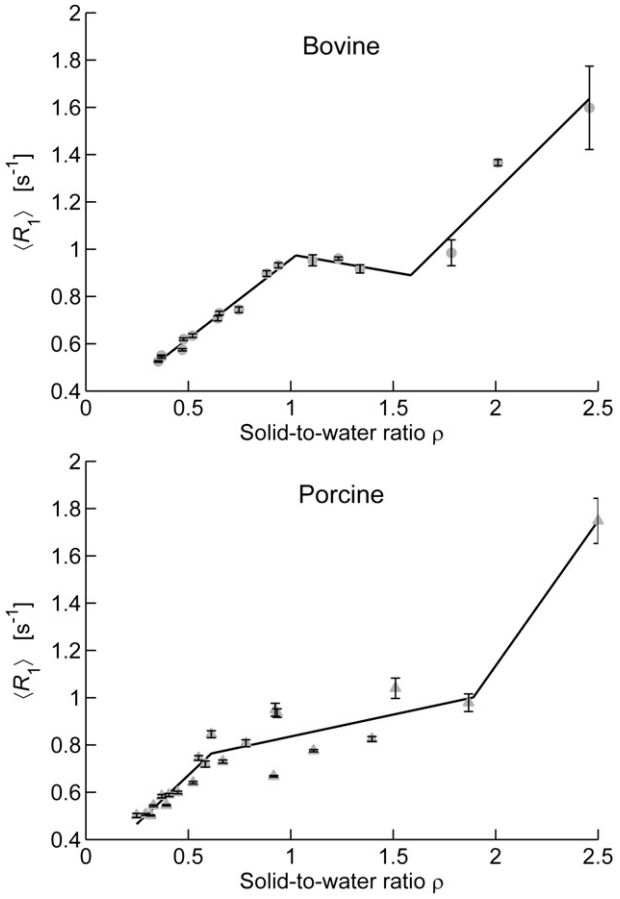

Fig. 3. Piecewise-linear regression of $\langle R_1 \rangle$ against solid-to-water ratio ρ for bovine (top) and porcine (bottom) data. Error bars represent 95% confidence intervals of the mean $\langle R_1 \rangle$ measured at each given ρ value.

latter hypothesis is very unlikely and therefore we should accept the piecewise-linear model as a better model than the linear model.

If these fits can be relied upon to indicate the correct trends, there are a number of points worth mentioning. In the first segment (highest water content) of both plots in Fig. 3 the intercepts are approximately equal ($\sim 0.27\ s^{-1}$) and clearly different to the intercepts recorded in Table II. These intercepts give a value of T_1 of approximately 3.7 s, which is much closer to our measured value for the T_1 of PBS, and this first segment almost certainly corresponds to the gradual loss of free or bulk water within the cartilage.

Using the scaled measure of water content

$$\frac{\rho_0}{\rho} = \frac{m^{\mathrm{w}}}{m_0^{\mathrm{w}}} \tag{7}$$

and using the average ρ_0 values for bovine and porcine of 0.364 and 0.297 respectively (w_0 values of 0.73 and 0.77 respectively), it appears from the plots in Fig. 3 (ρ_1 values in Table III) that the bulk water phases are depleted at 35% and 49% of the initial water masses for the bovine and porcine samples respectively. In other words, 65% of the total water of the bovine cartilage was free water, whereas only 51% of the porcine water was free water.

At the onset of the second segment, we see further differences between the bovine and porcine samples. These differences are in the intercept of this line and the extent (range of scaled water content) over which this segment exists. The intercepts recorded in Table III suggest values of T_1 of 0.9 s for bovine and 1.5 s for porcine. The larger porcine value also corresponds to the larger water content range of 33% (compared to the 12% range for the bovine samples — see ρ_1 and ρ_2 values in Table III and equation A.14). Since the ends of the range of these segments are somewhat uncertain, the above percentages should probably be regarded as underestimates. This segment is probably caused by water which is loosely bound to (or trapped in some way by) GAGs. The observed difference between the bovine and porcine data could reflect different concentrations of GAGs in these species or structural differences in the macromolecular content such as cross-linking.

Discussion

Ghiassi-Nejad *et al.*[18] have measured spin–spin relaxation times, T_2, in bovine articular cartilage as a function of hydration

Table III
Piecewise-linear regression values. Parameters $\{c_0, m_0\}$ refer to the intercept and slope of the first segment (the leftmost segment). $\{c_2, m_2\}$ refer to the third segment (the rightmost segment). The segment intercepts, ρ_i, [which can be calculated from $\{c_{i-1}, m_{i-1}\}$ and $\{c_i, m_i\}$] are the points at which the $(i-1)^{\mathrm{th}}$ segment meets the i^{th} segment

	Intercepts [s^{-1}]			Slopes [s^{-1}]			Segment intercepts	
	c_0	c_1	c_2	m_0	m_1	m_2	ρ_1	ρ_2
Bovine	0.286	1.127	−0.469	0.670	−0.149	0.856	1.03	1.59
Porcine	0.262	0.650	−1.320	0.819	0.185	1.227	0.61	1.89

Table IV
Comparison of the linear regression model and the piecewise-linear model on the separated bovine and porcine data of $\langle R_1 \rangle$ against ρ. r^2 is the goodness-of-fit parameter calculated as in equation 5, S_{res} is the sum of the square residuals, d_f is the degree of freedom, F is the F-test value, P is the P-value testing the hypothesis that the apparently better fit of the piecewise-linear model is due to chance

	Linear model			Piecewise-linear model			F	P
	r^2	S_{res}	d_f	r^2	S_{res}	d_f		
Bovine	0.931	0.0965	15	0.983	0.0240	11	8.31	0.0024
Porcine	0.826	0.276	20	0.940	0.0951	16	7.61	0.0013

level. They claim that from a ρ_0 of 0.333, free or bulk-like water becomes depleted at $\rho = 0.64$, and water associated with proteoglycans becomes depleted at $\rho = 2.7$. In terms of the scaled water content, 48% of the water is free and 40% is associated with proteoglycans. Whilst these percentages do not closely match our values for the bovine data, the porcine data is similar.

Furthermore, we can estimate the hydration coefficient for the water associated with this second segment. With the aid of equations A.13 and A.14, we can calculate the product $h^1\varsigma^1$ to be 0.34 for bovine and 1.11 for porcine (h^1 and ς^1 are the hydration coefficient for this water phase and the solids ratio of proteoglycans — see equations A.5 and A.6 for definitions). If we assume, as in[18] and as we have done above, that this segment is due to water loosely bound by GAGs, and that the solids ratio for this is $\varsigma^1 = 0.25$[18], then the hydration coefficient is 1.37 for bovine and 4.44 for porcine. In fact, the porcine cartilage was less mature than the bovine and it is generally observed that the GAG content of immature cartilage is higher than that of mature cartilage (see, for example, Reiter *et al.*[19]) and our own estimate (chemical assay) of GAG content in a similar porcine sample gave us $\varsigma^1 \approx 0.48$ (480 μg/mg). This would mean that the hydration coefficient for the porcine cartilage is probably less than 4.44 and could be closer to 2.3. Ghiassi-Nejad *et al.*'s measurements on bovine articular cartilage lead them to conclude that proteoglycans can bind as much as 4.7 g of water per gram of proteoglycans, with 3.6 g/g of that being loosely associated with proteoglycans. That is, hydration coefficients of 1.1 for the more tightly bound water and 3.6 for the loosely associated water. Again, our estimates for bovine cartilage do not closely match this value but the porcine value is more similar.

The third segment is much more uncertain than the previous two. If, however, the trends are correct, this segment indicates a departure from a simple fast-exchange model. The main point to observe is that the intercepts in this segment (for both plots) are negative and therefore this segment cannot correspond simply to the gradual depletion of one or more water phases (see the Appendix for an explanation of the fast-exchange model and its predictions).

Lüsse *et al.*[20] have also observed such a departure from the fast-exchange model when they measured proton spin–spin relaxation rates and deuterium spin–lattice relaxation rates of porcine articular cartilage by varying the osmotic pressure. They found a sharp rise in proton R_2 ($=1/T_2$) between solid-to-water ratios of approximately 1.0–1.5, and also a rise in the deuterium R_1 beginning at a solid-to-water ratio of approximately 1.8. The authors attributed this behaviour to changes in the cartilage as the macromolecular (solid) contents are brought into closer proximity. Such changes could affect the relaxation rates by a reduction in the mobility of the macromolecules and associated bound water, and also possibly due to changes in the quantities of bound water. While the rise in proton R_2 seems to occur during the second segment of our porcine data, the rise in deuterium R_1 does appear to approximately match the onset of our third segment where our measured $\langle R_1 \rangle$ seems to increase.

As mentioned above, some of the values quoted can only be regarded as indicative due to several possible sources of error. Firstly, we must acknowledge that there are very few data points contributing to some of the segments in Fig. 3, and this fact not only makes the fitting model uncertain but means that the fitting was sensitive to initial parameter estimates. Secondly, relaxation values were more uncertain the more the samples were dehydrated. There are two reasons for this: the most obvious is that lower water content samples provided noisier images from which to derive relaxation rates. The second reason is that as samples lost water, they became more rigid and tended to curl, often forming saddle geometries. In these shapes, the samples became very sensitive to vibrations and quite often motion artefacts could be observed in the images. These artefacts introduced a possible source of error into the determination of relaxation rates. We dealt with this latter source of error by eliminating data with severe artefacts and also by using the procedure described in the method section to reject pixels based on information from T_1, M_{eq} and r^2.

Despite the possible sources of error, references [18, 20] seem to corroborate our observations. If these observations are broadly correct, they might have consequences for both relaxation rate measurements and the mechanical properties of cartilage.

In terms of relaxation rates, whilst the linear regressions of Fig. 1 suggest that bovine and porcine data can be handled with a single formula, Fig. 3 suggests that this is not strictly true. The plot in Fig. 3 for the bovine data, in particular, causes us some concern. If the slope of the middle segment can be negative, as is observed in this plot, this implies that water content cannot be determined solely by spin–lattice relaxation measurements because the curve is no longer strictly increasing, that is, there is no longer a one-to-one correspondence.

The plots of Fig. 3 also suggest that the relative amounts of free and (loosely) bound water differ between the bovine and porcine articular cartilage studied in this work. It is well-known that water plays an important role in the tribological behaviour of cartilage and it is possible that the degree to which water is free, or trapped, or bound, also plays a role in the tribology. Furthermore, if the third segment is indeed a result of the closer packing of the macromolecular contents of cartilage, there might conceivably also be mechanical consequences at this stage of hydration.

Finally, we mention two recent papers by Reiter *et al.*[19,21]. The first of these papers derives water phase fractions in young and mature bovine nasal cartilage from multiexponential analysis of spin–spin relaxation. They observed two distinct relaxation times from which they derived estimates of what we have called here the loosely-bound water phase associated with proteoglycans. They found that this phase corresponded to 22% in the young cartilage and 31% in the mature cartilage. These values are similar to the values measured here (33% for porcine, 12% for bovine) but do not correlate with the GAG contents (per dry weight) in the same way. That is, the measurements reported herein show a higher proportion of this bound water phase being present in the porcine sample with its correspondingly higher GAG content — as one might intuitively expect — but in the abovementioned paper, the higher bound-water fraction is obtained from the mature cartilage with its lower GAG content. Apart from the fact that different types of cartilage samples were used in these two studies, there are a couple of possible reasons for this apparent discrepancy. As shown in Reiter *et al.*'s second paper[21], freeze-thawing can affect the cartilage microstructure and therefore the measured water phase fractions and, in the work presented here, cartilage samples were frozen after extraction and at other times during the experimental process. Also, because of the small number of data points contributing to the second segments in Fig. 3, the values we obtained for this water phase can only be regarded as estimates.

In summary, we have measured NMR spin–lattice relaxation rates $\langle R_1 \rangle$ of bovine and porcine articular cartilage as a function of water content (by freeze-drying). We have shown that if all the data are pooled together, linear correlations can be obtained between $\langle R_1 \rangle$ and inverse water content $1/w$ or the solid-to-water ratio ρ. However, when the bovine and porcine data are considered separately, deviations from linearity are seen and differences between these two data sets emerge. Interpreting the data in the context of the fast-exchange model allowed us to calculate estimates for the amount of free water and loosely-bound water in these samples. We found that in the bovine cartilage, 65% of the water was free and ~12% was loosely bound. In the porcine cartilage (which probably had a higher GAG content), 51% of the water was free and ~33% was loosely bound. The unaccounted percentages presumably correspond to water which is more tightly bound to GAGs and collagen.

Author contributions

All authors were involved in all stages of the work except data acquisition and analysis which was carried out by RAD and SSP.

Conflict of interest

There are no conflicts of interest.

Acknowledgements

This work was funded by EPSRC. It was partially funded through WELMEC, a Centre of Excellence in Medical Engineering funded by the Wellcome Trust and EPSRC, under grant number WT 088908/Z/09/Z and additionally supported by the NIHR (National Institute for Health Research) as part of a collaboration with the LMBRU (Leeds Musculoskeletal Biomedical Research Unit).

Appendix

Fast-exchange model of R_1 in cartilage

We describe a simplified model for the measured longitudinal relaxation rate R_1 of water in articular cartilage. We assume that the cartilage is composed of three dominant constituents; interstitial water, proteoglycans/GAGs, and collagen. We ignore, for example, intracellular water of the chondrocytes. Therefore, the interstitial water will be assumed to be free water (bulk-like water) or associated in some way to proteoglycans or to collagen. Water that is associated to a macromolecule can be tightly or directly-bound water, or water that is more loosely bound or trapped in some manner. We assume that it is valid to model the extracellular water in this discrete manner rather than using a continuous model and therefore assume that each of these phases can be assigned its own characteristic relaxation rate R_1. The fast-exchange model then assumes that the exchange rates between these phases are fast compared with the R_1 values of each phase. Evidence that the fast-exchange model is valid in, for example, canine articular cartilage can be found in the paper by Zheng and Xia[22].

The fast-exchange model predicts the measured relaxation rate R_1 to be a weighted sum of the individual relaxation rates

$$R_1 = \sum_{i=0}^{n} \varphi^i R_1^i \tag{A.1}$$

where the index i labels the water phases such that $i = 0$ is the free-water phase. R_1^i is the relaxation rate of phase i and φ^i is the mass-fraction of phase i, given by

$$\varphi^i = \frac{m^i}{m^{\mathrm{w}}} \tag{A.2}$$

where m^i is the mass of water in phase i and m^{w} is the total mass of water in the cartilage. The normalisation implies that

$$\sum_{i=0}^{n} \varphi^i = 1 \tag{A.3}$$

If we use this constraint to eliminate the free-water component from (A.1), we have

$$R_1 = R_1^0 + \sum_{i=1}^{n} \varphi^i \left(R_1^i - R_1^0 \right) \tag{A.4}$$

Let m^{si} be the mass of the solid giving rise to phase i (for $i = 1 \ldots n$). Since we are assuming that the solid mass is composed of only proteoglycans and collagen, $m^{\mathrm{s}} = m^{\mathrm{p}} + m^{\mathrm{c}}$, then $m^{si} = m^{\mathrm{p}}$ for n_{p} phases (the number of bound water phases associated with proteoglycans) and $m^{si} = m^{\mathrm{c}}$ for the remaining $n - n_{\mathrm{p}}$ phases. In general, we can define a solids ratio

$$\varsigma^i = \frac{m^{si}}{m^{\mathrm{s}}} \tag{A.5}$$

which will either be equal to the proteoglycan value ς or the collagen value ς^{c}, where $\varsigma^{\mathrm{c}} = 1 - \varsigma^{\mathrm{p}}$.

Let us also define hydration coefficients, h^i, such that the mass of bound water in phase i is proportional to the solid mass giving rise to that phase, by

$$m^i = h^i m^{si} \tag{A.6}$$

Using the solids ratio and the hydration coefficients, we can express the bound water mass-fractions as

$$\varphi^i = h^i \varsigma^i \rho \tag{A.7}$$

and we can then express R_1 in terms of ρ

$$R_1 = R_1^0 + \rho \sum_{i=1}^{n} h^i \varsigma^i \left(R_1^i - R_1^0 \right) \tag{A.8}$$

Therefore, under the assumption that the free water ($i = 0$) is lost before any other water phase (but while some free water still remains), the relaxation rate should be linearly-dependent on the solid-to-water ratio ρ and the intercept of this line is the relaxation rate of the free-water phase. Note that using the water content defined by equations 2 and 3, (A.8) becomes

$$R_1 = R_1^0 + \frac{1}{w} \frac{1}{(1 + 1/\rho_0)} \sum_{i=1}^{n} h^i \varsigma^i \left(R_1^i - R_1^0 \right) \tag{A.9}$$

and it can be seen (under the same assumptions as above) that the measured relaxation rate is linear in $1/w$ with a slope modified by the factor $1/(1 + 1/\rho_0)$ but with the same intercept. We note that, using equation 3, the above factor can be alternatively written as $1 - w_0$.

Depletion of free water

At the point when the free water has been fully depleted, the remaining water is all bound. Therefore the total mass of water is given by

$$m^{\mathrm{w}} = \sum_{i=1}^{n} h^i m^{si} \tag{A.10}$$

which provides the upper limit of validity on ρ. That is, (A.8) is valid for

$$\rho_0 \leq \rho \leq \frac{1}{\sum_{i=1}^{n} h^i \varsigma^i} \tag{A.11}$$

Beyond this point (A.8) is no longer valid because the free-water phase plays no role in the subsequent relaxation behaviour. The free-water phase therefore drops out of equations (A.1), (A.3) and (A.4). Let us assume that as further water is lost from the cartilage, it is purely from the $i=1$ phase (assumed to be the most loosely-bound phase). (A.8) then becomes

$$R_1 = R_1^1 + \rho \sum_{i=2}^{n} h^i \varsigma^i \left(R_1^i - R_1^1\right) \tag{A.12}$$

The measured relaxation rate is again linear in ρ but the slope has changed and the intercept (with the $\rho=0$ axis) is now the relaxation rate of the $i=1$ phase. If this logic is continued, whereby we deplete one phase at a time, the curve is seen to be piecewise-linear with $n+1$ segments. The intercepts of the lines describing each segment are the relaxation rates of the phase being depleted and should therefore always be positive.

If we define $\rho_j\,(j>0)$ as the point at which the $(j-1)^{\text{th}}$ phase has been fully depleted and the j^{th} phase is about to begin depletion, then it can be shown that

$$\frac{1}{\rho_j} - \frac{1}{\rho_{j+1}} = h^j \varsigma^j \tag{A.13}$$

If we multiply this value by the fully-hydrated solid-to-water ratio ρ_0 we obtain the mass-fraction for phase j for the fully-hydrated cartilage

$$\frac{\rho_0}{\rho_j} - \frac{\rho_0}{\rho_{j+1}} = \frac{m^j}{m_0^{\text{w}}} = \varphi_0^j \tag{A.14}$$

References

1. Greene GW, Zappone B, Zhao B, Söderman O, Topgaard D, Rata G, *et al.* Changes in pore morphology and fluid transport in compressed articular cartilage and the implications for joint lubrication. Biomaterials 2008;29:4455–62.
2. Juras V, Szomalanyi P, Majdisova Z, Trattnig S. MR-compatible compression device for in-vitro evaluation of biomechanical properties of cartilage. J Biomech Sci Eng 2008;3:200–8.
3. Nieminen MT, Töyräs J, Laasanen MS, Silvennoinen J, Helminen HJ, Jurvelin JS. Prediction of biomechanical properties of articular cartilage with quantitative magnetic resonance imaging. J Biomech 2004;37:321–8.
4. Nissi MJ, Rieppo J, Töyräs J, Laasanen MS, Kiviranta I, Nieminen MT, *et al.* Estimation of mechanical properties of articular cartilage with MRI – dGEMRIC, T-2 and T-1 imaging in different species with variable stages of maturation. Osteoarthritis Cartilage 2007;15:1141–8.
5. Kneeland JB, Reddy R. Frontiers in musculoskeletal MRI: articular cartilage. J Magn Reson Imaging 2007;25:339–44.
6. Recht MP, Goodwin DW, Winalski CS, White LM. MRI of articular cartilage: revisiting current status and future directions. Am J Roentgenol 2005;185:899–914.
7. Gu KB, Li LP. A human knee joint model considering fluid pressure and fiber orientation in cartilages and menisci. Med Eng Phys 2011;33:497–503.
8. Lahm A, Mrosek E, Spank H, Erggelet C, Kasch R, Esser J, *et al.* Changes in content and synthesis of collagen types and proteoglycans in osteoarthritis of the knee joint and comparison of quantitative analysis with Photoshop-based image analysis. Arch Orthop Trauma Surg 2010;130:557–64.
9. Maroudas A. Physicochemical properties of articular cartilage. In: Freeman MAR, Ed. Adult Articular Cartilage. Kent, England: Pitman Medical Publishing Co; 1979:215–90.
10. Venn M, Maroudas A. Chemical composition and swelling of normal and osteoarthrotic femoral-head cartilage .1. Chemical composition. Ann Rheum Dis 1977;36:121–9.
11. Burstein D, Velyvis J, Scott KT, Stock KW, Kim YJ, Jaramillo D, *et al.* Protocol issues for delayed Gd(DTPA)(2-)-enhanced MRI: (dGEMRIC) for clinical evaluation of articular cartilage. Magn Reson Med 2001;45:36–41.
12. Chen CA, Kijowski R, Shapiro LM, Tuite MJ, Davis KW, Klaers JL, *et al.* Cartilage morphology at 3.0T: assessment of three-dimensional magnetic resonance imaging techniques. J Magn Reson Imaging 2010;32:173–83.
13. Gründer W, Kanowski M, Wagner M, Werner A. Visualization of pressure distribution within loaded joint cartilage by application of angle-sensitive NMR microscopy. Magn Reson Med 2000;43:884–91.
14. Souza RB, Stehling C, Wyman BT, Hellio Le Graverand M-P, Li X, Link TM, *et al.* The effects of acute loading on T1rho and T2 relaxation times of tibiofemoral articular cartilage. Osteoarthritis Cartilage 2010;18:1557–63.
15. Gründer W. MRI assessment of cartilage ultrastructure. NMR Biomed 2006;19:855–76.
16. Momot KI, Pope JM, Wellard RM. Anisotropy of spin relaxation of water protons in cartilage and tendon. NMR Biomed 2010;23:313–24.
17. Berberat JE, Nissi MJ, Jurvelin JS, Nieminen MT. Assessment of interstitial water content of articular cartilage with T-1 relaxation. Magn Reson Imaging 2009;27:727–32.
18. Ghiassi-Nejad M, Torzilli PA, Peemoeller H, Pintar MM. Proton spin–spin relaxation study of molecular dynamics and proteoglycan hydration in articular cartilage. Biomaterials 2000;21:2089–95.
19. Reiter DA, Roque RA, Lin PC, Irrechukwu O, Doty S, Longo DL, *et al.* Mapping proteoglycan-bound water in cartilage: improved specificity of matrix assessment using multi-exponential transverse relaxation analysis. Magn Reson Med 2011;65:377–84.
20. Lüsse S, Knauss R, Werner A, Gründer W, Arnold K. Action of compression and cations on the proton and deuterium relaxation in cartilage. Magn Reson Med 1995;33:483–9.
21. Reiter DA, Peacock A, Spencer RG. Effects of frozen storage and sample temperature on water compartmentation and multi-exponential transverse relaxation in cartilage. Magn Reson Imaging 2011;29:561–7.
22. Zheng SK, Xia Y. Multi-components of T-2 relaxation in ex vivo cartilage and tendon. J Magn Reson 2009;198:188–96.